Jurnal Ilmu Fisika
Vol. 19, No. 1, March 2027, pp. 29–39
ISSN: 1979-4657 (Print); 2614-7386 (Online)
https://doi.org/10.25077/jif.19.1.29-39.2027

Jurnal Ilmu Fisika
Open Access

Association of Tube Current-Time Product with Quantitative CT Image Quality in Bone Scan SPECT/CT

Fransischa Ramona[1], Afdhal Muttaqin[1*], Yola Despriani[2]

[1] Department of Physics, Faculty of Mathematics and Natural Sciences, Universitas Andalas, Padang, 25163, Indonesia
[2] Nuclear Medicine Sub-Division, Department of Radiology, Radiotherapy, and Nuclear Medicine, Dr. M. Djamil Hospital, Padang, 25217, Indonesia

Article Info

Article History:

Received September 9, 2026
Revised October 30, 2026
Accepted October 31, 2026
Published online November 07, 2026

Keywords:

automatic exposure control
bone scan
computed tomography
signal-to-noise ratio
tube current-time product

Corresponding Author:

Afdhal Muttaqin,
Email: afdhalmuttaqin@sci.unand.ac.id

ABSTRACT

In bone scan single-photon emission computed tomography/computed tomography (SPECT/CT), the CT provides the anatomical reference for localizing scintigraphic findings. Because automatic exposure control (AEC) modulates the tube current–time product (mAs) according to patient attenuation, CT image quality may differ between examinations. This study quantified CT image quality and examined its association with AEC-selected mAs. CT datasets from 72 patients at the Nuclear Medicine Unit of Dr. M. Djamil Hospital, Padang, were analyzed retrospectively. Mean CT number and image noise were measured in a hepatic region of interest to derive signal-to-noise ratio (SNR), and data were evaluated using correlation and simple linear regression. Mean mAs, liver CT attenuation, image noise, and SNR were 58.35 ± 16.24, 56.66 ± 8.55 HU, 2.14 ± 0.49 HU, and 27.57 ± 6.59, respectively. Body mass index (BMI) correlated positively with mAs ($r = 0.642$, $p < 0.001$). Moderate negative correlations were found between mAs and SNR ($r = -0.468$, $p < 0.001$) and between mAs and liver CT attenuation ($\rho = -0.444$, $p < 0.001$), whereas mAs and image noise were not significantly associated ($\rho = 0.209$, $p = 0.078$). Under AEC, mAs alone cannot adequately explain variability in quantitative CT image quality.

Copyright © 2026 Author(s)

1. INTRODUCTION

Hybrid single-photon emission computed tomography/computed tomography (SPECT/CT) now occupies a central place in nuclear medicine, a discipline whose diagnostic scope has widened considerably with advances in radiopharmaceuticals and imaging instrumentation (Vaz et al., 2020). By coupling the functional information of SPECT with the anatomical detail of computed tomography (CT) (Bouchareb et al., 2024), the technique allows foci of abnormal tracer uptake on bone scintigraphy to be localized and characterized against the underlying skeletal anatomy, and this complementary information has made SPECT/CT a mainstay of hybrid skeletal imaging (Ziessman et al., 2014; Lee & Joo, 2025). The diagnostic value of the CT component, however, rests on the quality of the images it produces, which in turn depends largely on the tube current–time product (mAs), the quantity that governs X-ray output during acquisition. The present work addresses this relationship directly, examining how the mAs delivered during routine bone scan SPECT/CT relates to objective, quantitative measures of CT image quality.

Bone scintigraphy remains one of the most frequently performed examinations for evaluating skeletal disease, particularly in patients with suspected or established osseous metastases (Ben-Rejeb &

Attribution-NonCommercial 4.0 International

Ben-Sellem, 2022). Technetium-99m methylene diphosphonate (^{99m}Tc-MDP) is commonly employed for this purpose owing to its affinity for sites of increased osteoblastic activity (Wyngaert et al., 2016; Bartel et al., 2018). Within a SPECT/CT examination, the CT acquisition serves a dual role: it furnishes anatomical correlation and may also supply the attenuation information used for SPECT attenuation correction (Verfaillie et al., 2023). The CT images must therefore be of sufficient quality for both tasks. Every CT acquisition, however, adds to the radiation burden of the patient, so acquisition parameters must be selected judiciously if adequate image quality is to be achieved without unwarranted exposure (Tulik et al., 2020; Alrehily & Alshamrani, 2023).

In the CT component, both radiation dose and image quality are governed by technical factors, notably tube potential and mAs, together with patient-related factors such as body size and tissue attenuation. The mAs determines the number of X-ray photons generated during acquisition and is thus a principal determinant of image noise; raising the mAs increases the photon flux reaching the detector and, other conditions being equal, lowers noise (Sadia et al., 2024). Earlier investigations have shown that CT acquisition parameters can be optimized to reduce radiation exposure while preserving appropriate image quality (Gupta et al., 2017; Tulik et al., 2020; Alezzi et al., 2026).

In clinical practice, the tube current is seldom held constant. Automatic exposure control (AEC), also termed automatic tube current modulation (ATCM), adapts the tube current to patient attenuation so that a predefined level of image quality is maintained while radiation exposure is kept in check (Vañó et al., 2017; Tsalafoutas et al., 2024). On the Siemens Symbia Intevo Bold system, this function is performed by the CARE Dose4D algorithm, which first estimates patient attenuation from the topogram and then modulates the tube current longitudinally and angularly during acquisition, drawing on the topogram data together with real-time attenuation measurements obtained as the gantry rotates (McMillan et al., 2017; Inoue et al., 2022). As a result, the delivered mAs may differ substantially among patients undergoing an identical protocol. Although a higher mAs generally improves photon statistics and can suppress image noise, the final image quality is also shaped by the characteristics of the individual patient (Sulayman et al., 2025). Examining how AEC-selected mAs relates to an objective, quantitative image-quality metric could therefore clarify the sources of image-quality variability encountered under clinical conditions.

Objective CT image quality can be quantified with metrics such as the signal-to-noise ratio (SNR) (Hoeijmakers et al., 2025). In this study, SNR was defined as the mean CT attenuation (CT number) within a region of interest (ROI) divided by the standard deviation of attenuation within the same ROI, the latter serving as the measure of image noise (Yoon et al., 2021; Arjah et al., 2026). Defined in this way, SNR is a composite index that depends jointly on tissue attenuation and image noise. A change in SNR between examinations may thus arise from a change in either quantity, and its interpretation must take account of both the acquisition conditions and the attenuation properties of the tissue being measured (Sookpeng & Butdee, 2017).

Although the influence of mAs on CT image quality has been investigated extensively, comparatively little is known about how AEC-selected mAs relates to quantitative image-quality parameters in clinical bone scan SPECT/CT. Because the mAs is adjusted automatically according to patient attenuation and acquisition conditions, its relationship with SNR may depart from that observed when exposure is fixed. The present study was therefore designed to characterize CT image quality quantitatively, in terms of liver CT attenuation, image noise, and SNR, and to investigate how these parameters relate to the AEC-selected tube current–time product in patients undergoing bone scan SPECT/CT. The findings are intended to provide quantitative evidence on image-quality variability under AEC operation that may inform the further evaluation and optimization of CT acquisition protocols.

2. METHOD

2.1 Study Design and Data Collection

This retrospective study drew on data from the Nuclear Medicine Unit, Department of Radiology, Radiotherapy, and Nuclear Medicine, RSUP Dr. M. Djamil, Padang, collected between

March and May 2026. Examinations were eligible for inclusion when complete demographic data, CT images, and the acquisition parameters required for quantitative image-quality assessment were available; those with incomplete demographic or imaging records were excluded. In total, 72 patients fulfilled these criteria and were included in the analysis. Age, sex, body weight, height, and body mass index (BMI) were recorded where available, with BMI calculated as body weight in kilograms divided by the square of height in meters (kg/m²).

2.2 CT Image Acquisition Protocol

All CT acquisitions were performed on a Siemens Symbia Intevo Bold SPECT/CT system at a fixed tube voltage of 130 kVp and a pitch of 1.5, and images were reconstructed at a slice thickness of 5.0 mm. The tube current–time product was modulated automatically by Siemens CARE Dose4D in accordance with patient attenuation. No intravenous contrast medium was administered in any examination.

2.3 Quantitative Evaluation of CT Image Quality

CT image quality was evaluated quantitatively in terms of SNR measured within the liver. The liver was chosen as the reference region because its relatively homogeneous soft-tissue parenchyma can be identified reproducibly on CT images and lends itself to quantitative assessment of attenuation and noise (Jaruvongvanich et al., 2024; Lin et al., 2024). A circular ROI 13 px (12.70 mm) in diameter was placed within homogeneous parenchyma of the right hepatic lobe, avoiding visible vessels and image artifacts. To limit measurement variability, identical ROI dimensions and placement criteria were applied to every examination. SNR was calculated as:

$$SNR = \frac{Signal}{Noise} \tag{1}$$

where *signal* is the mean CT number within the liver ROI (HU), and *noise* is the standard deviation of the CT numbers within the same ROI (HU). All measurements were performed with IndoQCT software (version 26d.4). The measured liver CT numbers were additionally compared with the range reported in the literature for normal hepatic tissue.

2.4 Statistical Analysis

Descriptive statistics were used to summarize patient characteristics, BMI, liver CT number, image noise, SNR, and mAs, with continuous variables expressed as mean ± standard deviation (SD) and range. The normality of each continuous variable entering the correlation analysis (BMI, mAs, SNR, liver CT number, and image noise) was examined with the Shapiro–Wilk test. Pearson's correlation coefficient (r) was applied to the BMI–mAs and mAs–SNR pairs, for which the normality assumption was satisfied. For the associations of mAs with liver CT attenuation and with image noise, where this assumption was violated, Spearman's rank correlation coefficient (ρ) was used instead. Correlation coefficients were interpreted in terms of both direction and strength, and $p < 0.05$ was considered statistically significant. Simple linear regression was then used to characterize the relationships of mAs with BMI, SNR, liver CT number, and image noise, and the coefficient of determination (R^2) was used to express the proportion of variance accounted for by each regression model.

2.5 Ethical Approval

This study received ethical approval from the Health Research Ethics Committee of RSUP Dr. M. Djamil Hospital, Padang, Indonesia (Ethical Clearance No. DP.04.03/D/XVI.10.1/152/2026, issued on April 13, 2026).

3. RESULTS AND DISCUSSION

3.1 Patient Characteristics and the Relationship Between BMI and Tube Current–Time Product

Seventy-two patients who underwent bone scan SPECT/CT were included in the study. The cohort comprised 37 men (51.4%) and 35 women (48.6%), a nearly equal sex distribution. Mean age

was 60.01 ± 12.92 years (range, 35-84 years), a span typical of the adult population referred for bone scan SPECT/CT in routine practice. Taken together, the balanced sex distribution and wide age range point to a heterogeneous study population. Mean body weight and height were 56.74 ± 10.25 kg and 157.42 ± 7.30 cm, respectively, and mean BMI was 22.91 ± 3.91 kg/m² (range, 13.67-34.23 kg/m²). The demographic characteristics of the cohort are summarized in Table 1.

Table 1 Patient characteristics.

Characteristics	Value
Number of patients	72
Male	37 (51.4%)
Female	35 (48.6%)
Age, mean ± SD (years)	60.01 ± 12.92
Age, range (years)	35 - 84
Weight (kg) mean ± SD	56.74 ± 10.25
Weight, range (kg)	35 - 84
Height (cm) mean ± SD	157.42 ± 7.30
Height, range (cm)	144 - 178
BMI (kg/m^2) mean ± SD	22.91 ± 3.91
BMI, range (kg/m^2)	13.67 - 34.23

Inter-individual differences in body size can alter the tube current selected by the AEC system, and hence the delivered mAs, with downstream effects on image noise and SNR. These characteristics thus provide essential context for interpreting the variation in acquisition parameters and quantitative image-quality metrics observed here. The association between BMI and mAs was examined by Pearson's correlation analysis, which revealed a strong, statistically significant positive correlation (r = 0.642, $p < 0.001$). Linear regression likewise showed mAs rising with BMI (Figure 1), with a coefficient of determination (R^2) of 0.4334, indicating that BMI accounted for 43.34% of the variance in mAs. In other words, patients with a higher BMI tended to receive a higher AEC-selected mAs.

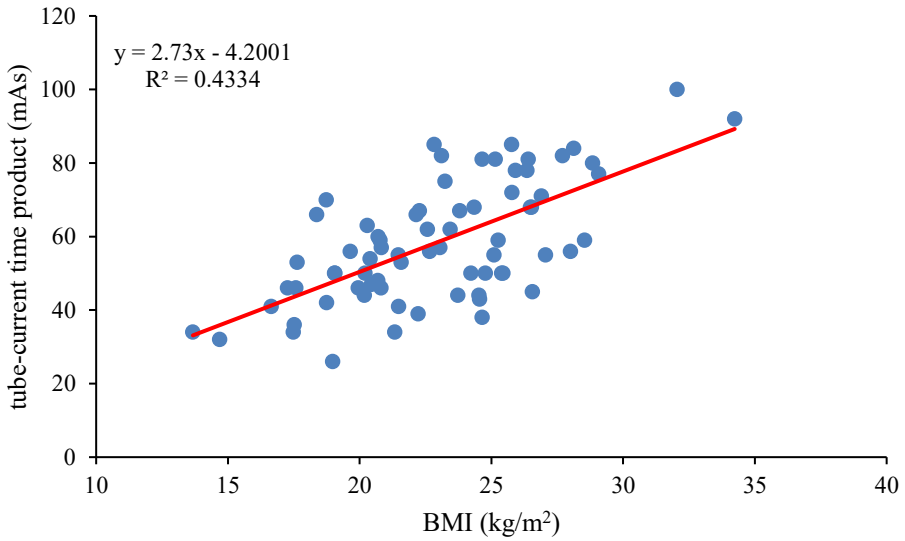


Figure 1 Linear regression analysis of the relationship between body mass index (BMI) and tube current–time product (mAs) in patients undergoing bone scan SPECT/CT.

This positive association is consistent with the operating principle of AEC, which adjusts the tube current automatically to patient attenuation in order to preserve the target image quality. The exposure, defined as the product of tube current (mA) and exposure time (s), is modulated both along the scan axis and around the patient to compensate for regional differences in tissue attenuation (Martin

& Sookpeng, 2016). The resulting modulation pattern therefore mirrors the body shape and anatomical configuration of each patient. Patients of greater body thickness attenuate a larger fraction of the X-ray beam and generally require a higher mAs to sustain adequate photon statistics and keep image noise under control (Martin & Sookpeng, 2016; Inoue et al., 2018; Sulayman et al., 2025). The elevated mAs observed in patients with higher BMI is thus best understood as the response of the exposure control system to increased attenuation, rather than as an independently selected increase in tube current.

Although the correlation was strong and statistically significant, BMI explained only 43.34% of the variance in mAs. Part of the unexplained variance may stem from discrepancies between the BMI values reported by some patients and their actual body habitus at the time of scanning. Such discrepancies were suspected on visual review of the CT images, in which the apparent body habitus of certain patients did not correspond to their recorded BMI. Inaccurate anthropometric data of this kind would introduce measurement error and weaken the observed BMI–mAs relationship. Measuring body weight and height on the day of examination is therefore advisable to obtain more reliable BMI values.

Despite these uncertainties, the CT dose reports confirmed that the AEC system adjusted the mAs to the physical characteristics of each patient during scanning. Patients classified as underweight received lower mAs than those classified as normal weight or overweight, indicating that tube current modulation responded to patient attenuation even where the reported BMI category may not have reflected the true body habitus. Because such discrepancies may have reduced the reliability of the BMI–mAs analysis, mAs was subsequently treated as a recorded acquisition parameter capturing the response of the AEC system under routine clinical conditions, and its relationship with image quality was examined on that basis. Under otherwise constant operating conditions, the mAs is proportional to the number of X-ray photons produced. Since photon quantity is a primary determinant of image noise, mAs constitutes a key parameter in the evaluation of CT image quality. The analysis that follows therefore examines how variation in AEC-selected mAs relates to quantitative image quality in routine clinical examinations.

3.2 Quantitative Evaluation of CT Image Quality

Quantitative image quality was assessed within a hepatic ROI in terms of liver CT number, image noise, and SNR; the results are summarized in Table 2.

Table 2 Quantitative CT image-quality parameters.

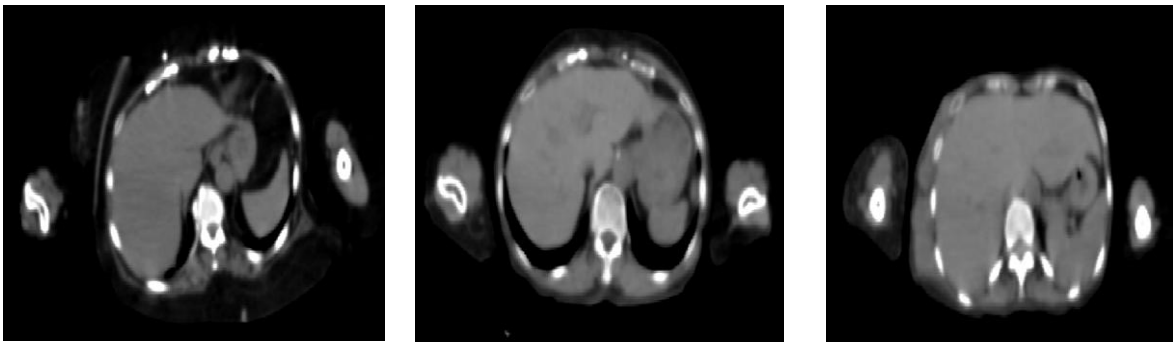
Parameter	Minimum	Maximum	Mean ± SD
Tube current-time product (mAs)	26	100	58.35 ± 16.24
CT number liver (HU)	29.64	72.97	56.66 ± 8.55
Noise (HU)	1.31	3.85	2.14 ± 0.49
SNR	13.83	44.10	27.57 ± 6.59

Liver CT numbers ranged from 29.64 to 72.97 HU, with a mean of 56.66 ± 8.55 HU. This mean lies within the reference range of approximately 50-70 HU reported for normal hepatic parenchyma (Dance et al., 2014), suggesting that hepatic attenuation in the study population was, on the whole, within expected limits. Several individual values nevertheless fell outside this range, which may be attributable to inter-individual differences in patient characteristics and tissue composition, as well as to tube voltage and scanner-related factors (Dance et al., 2014).

Image noise averaged 2.14 ± 0.49 HU (range, 1.31–3.85 HU), and SNR averaged 27.57 ± 6.59 (range, 13.83–44.10). The relatively high SNR indicates that the hepatic signal was well separated from the background noise, allowing hepatic anatomical structures to be clearly delineated; in general, a higher SNR makes the signal easier to distinguish from noise (Anthon et al., 2025). Inter-patient variation in noise and SNR may be linked to differences in mAs, which the AEC system adjusted automatically to patient attenuation. Differences in anatomy and attenuation among patients would thus give rise to different mAs values and, in turn, to different noise and SNR levels.

Figure 2 illustrates this inter-patient variation in SNR with representative CT images, selected to span the observed range of mAs and SNR values. The three cases differ markedly. Patient (a) was scanned at 78 mAs and had an SNR of 13.83, patient (b) at 54 mAs with an SNR of 26.10, and patient

(c) at 41 mAs with an SNR of 44.10. Under AEC operation, then, a higher mAs did not necessarily yield a higher SNR: the highest mAs (78 mAs) was accompanied by the lowest SNR (13.83), whereas the lowest mAs (41 mAs) coincided with the highest SNR (44.10). This inverse pattern is consistent with the way AEC operates, raising the mAs in response to patient attenuation, so that a high mAs value may simply signal greater x-ray attenuation by the patient. These observations suggest that, in routine clinical AEC operation, mAs alone may not adequately characterize quantitative CT image quality.



(a) (b) (c)

Figure 2 Representative liver CT images from patients with different tube current–time products and SNR values: (a) 78 mAs, SNR = 13.83; (b) 54 mAs, SNR = 26.10; (c) 41 mAs, SNR = 44.10.

3.3 Relationship Between Tube Current-Time Product and CT Image Quality Parameters

Normality was assessed with the Shapiro–Wilk test. SNR ($p = 0.660$) and mAs ($p = 0.154$) were normally distributed, so the association between them was evaluated with Pearson's correlation. Liver CT number ($p < 0.001$) and image noise ($p = 0.021$), by contrast, deviated from normality, and their associations with mAs were therefore assessed with Spearman's rank correlation. The results of the correlation analyses are presented in Table 3.

Table 3 Correlation between tube current–time product (mAs) and CT image-quality parameters.

Association	Method	n	Correlation coefficient (r/ρ)	p-value
mAs with SNR	Pearson	72	-0.468	<0.001
mAs with CT number Liver	Spearman	72	-0.444	<0.001
mAs with noise	Spearman	72	0.209	0.078

Pearson's analysis revealed a moderate, statistically significant negative correlation between AEC-selected mAs and SNR ($r = -0.468$, $p < 0.001$); examinations performed at higher mAs thus tended to exhibit lower SNR. This relationship was further characterized by simple linear regression (Figure 3). Because all examinations were acquired with AEC, the mAs was itself a function of patient attenuation. Patients who required a higher tube output are therefore likely to have had greater attenuation, and possibly other characteristics, that also influenced the measured SNR.

The negative regression slope in Figure 3 agrees in direction with the Pearson coefficient, confirming an inverse linear association between mAs and predicted SNR. The coefficient of determination, however, was only 0.2189, indicating that mAs accounted for a relatively small proportion of the variability in SNR under AEC conditions. The remaining variance is likely attributable to patient- and acquisition-related factors that were not fully captured in this study.

This association must be interpreted in light of how AEC operates. Here, mAs was analyzed as a recorded acquisition parameter reflecting the response of the AEC system in routine practice, not as an independently controlled exposure variable. Because the system adjusts the tube current to patient attenuation, a high mAs value is more plausibly an indicator of greater attenuation than of a deliberate increase in tube output. The negative association observed here therefore does not imply that increasing mAs directly reduces SNR. Moreover, since SNR was calculated as the ratio of the mean to the standard

deviation of CT attenuation within the same liver ROI, variation in SNR may arise from either term, and the lower SNR at higher mAs should not be read simply as a deterioration in image noise or in overall image quality. Taken together, these results indicate that quantitative image quality under AEC cannot be adequately characterized by mAs alone, and that other patient-related and technical factors contribute to the observed variation.

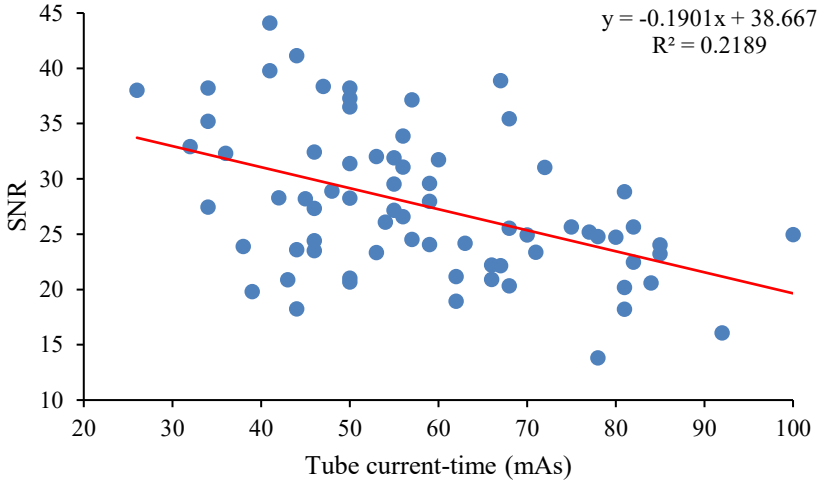


Figure 3 Linear regression between tube current–time product (mAs) and signal-to-noise ratio (SNR).

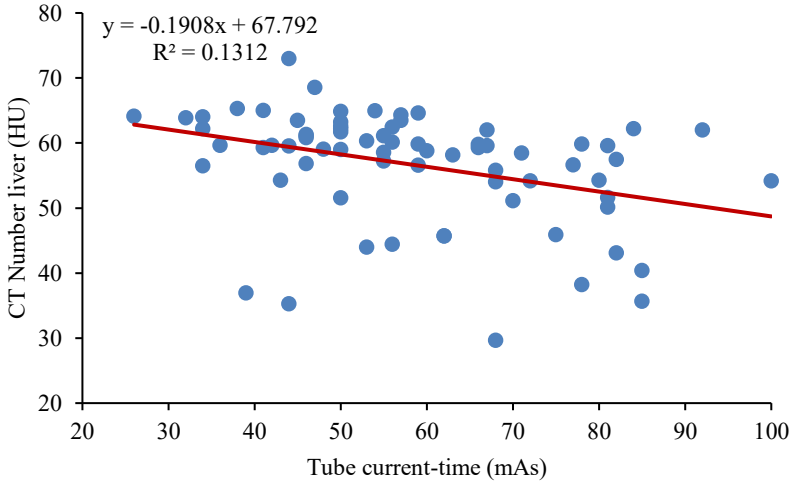


Figure 4 Linear regression between tube current–time product (mAs) and liver CT number.

Figure 4 depicts the relationship between mAs and liver CT number, expressed in Hounsfield units (HU). The negative slope indicates an inverse association, confirmed by a statistically significant negative correlation ($\rho = -0.444$, $p < 0.001$): higher mAs values tended to coincide with lower liver CT numbers. Despite this statistical significance, the regression yielded an R^2 of only 0.1312, so mAs explained a small fraction of the variability in liver CT number. Factors other than mAs, including differences in patient characteristics, hepatic tissue composition, and acquisition conditions, therefore appear to contribute substantially to this variability and may underlie the observed negative correlation.

The relationship between mAs and image noise is shown in Figure 5. Spearman's rank correlation revealed a weak positive association ($\rho = 0.209$) that did not reach statistical significance ($p = 0.078$). Although the positive regression slope matched the direction of the correlation coefficient, the R^2 of 0.0637 indicates that mAs accounted for only a small proportion of the variability in noise. Because AEC adjusts the tube current according to patient attenuation and the exposure-control strategy of the

scanner, patients assigned a higher mAs are also likely to present greater attenuation, which can leave higher residual noise despite the increased tube current (Danielsson et al., 2021). This interpretation is partly in line with the observations of Sookpeng et al. (2014), who reported that image noise increased with patient size on certain Siemens scanners equipped with ATCM, although no such correlation was evident under other scanner conditions.

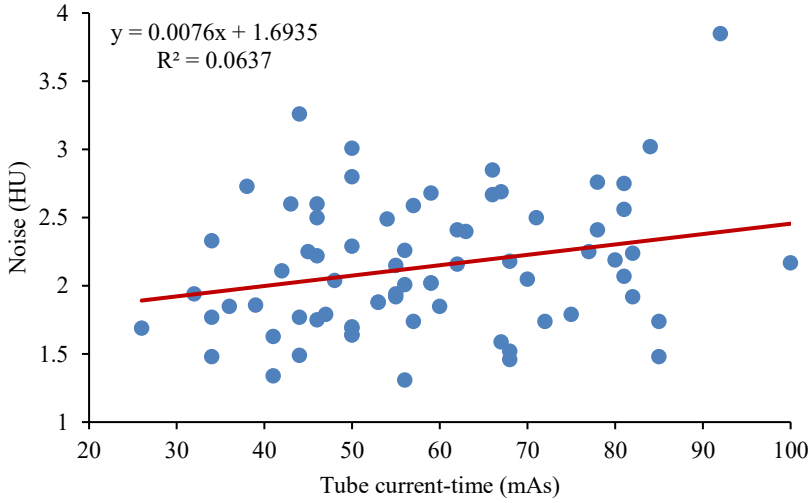
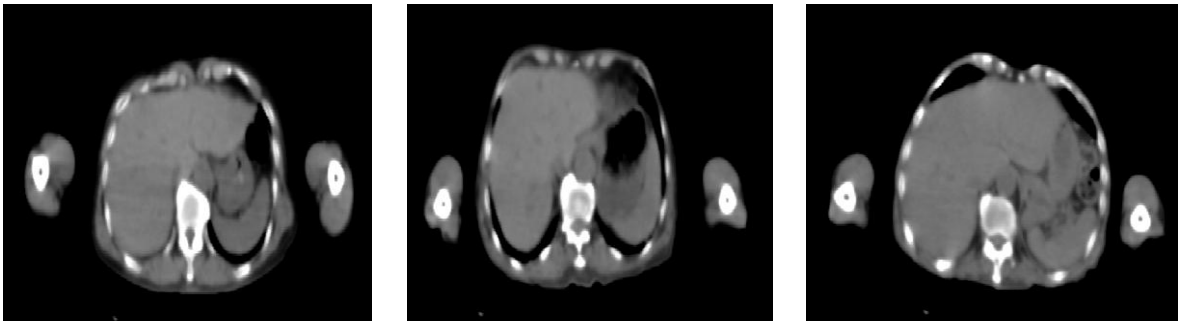


Figure 5 Linear regression between tube current–time product (mAs) and image noise.

To explore further the contribution of patient-specific characteristics to image quality, images from three patients scanned at the same mAs were compared (Figure 6). Although all three examinations were acquired at 50 mAs, their SNR values differed; the corresponding liver CT numbers and noise values are listed in Table 4.



(a) (b) (c)

Figure 6 Representative liver CT images from three patients scanned at an identical tube current–time product of 50 mAs, showing different SNR values: (a) SNR = 37.29; (b) SNR = 36.51; (c) SNR = 31.39.

Table 4 SNR variation among examinations acquired at the same tube current–time product (mAs).

Parameters	Image (a)	Image (b)	Image (c)
Tube current-time product (mAs)	50	50	50
Liver CT number (HU)	63.23	61.70	51.70
Noise (HU)	1.70	1.69	1.64
SNR	37.29	36.51	31.39

The comparison in Figure 6 shows that mAs alone did not determine the measured SNR. At an identical 50 mAs, SNR ranged from 31.39 to 37.29 across the three examinations. Notably, the examination with the lowest SNR did not exhibit the highest noise; instead, it had the lowest liver CT

number (51.70 HU). Under the SNR definition adopted here, variation in SNR can therefore originate from changes in the mean liver CT number (the numerator) as well as in image noise (the denominator).

As shown in Figure 6 and Table 4, image (a) had a liver CT number of 63.23 HU and noise of 1.70 HU, yielding an SNR of 37.29, while image (b) had corresponding values of 61.70 HU and 1.69 HU, giving an SNR of 36.51. Image (c), in contrast, combined the lowest liver CT number (51.70 HU) with the lowest noise (1.64 HU), yet had the lowest SNR (31.39). Its reduced SNR thus stemmed primarily from lower hepatic attenuation rather than from increased noise. These cases demonstrate that, even at a fixed mAs, the measured SNR can vary with differences in mean CT attenuation and image noise, which may in turn reflect patient-specific anatomy, body composition, and x-ray attenuation.

Several limitations of this study should be acknowledged. First, the data were obtained from a single center using one SPECT/CT system, which may limit the generalizability of the findings to other institutions, scanner models, and acquisition protocols. Second, the retrospective design of the study precludes control over patient selection and data acquisition conditions, and may introduce selection bias. Third, BMI was the only available indicator of patient size; it does not fully represent cross-sectional anatomy or x-ray attenuation, and direct measures such as patient diameter were not evaluated. Moreover, uncertainty in anthropometric measurements, such as variability in recorded height and weight, may have affected the accuracy of BMI calculation. Fourth, image quality was assessed solely by quantitative SNR, without complementary qualitative evaluation by radiologists, nuclear medicine physicians, or other qualified observers. Furthermore, multivariable analysis was not performed, limiting the ability to account for potential confounding factors that were not measured or included in the analysis.

4. CONCLUSION

In bone scan SPECT/CT, the CT images exhibited a mean liver CT attenuation of 56.66 ± 8.55 HU and a mean SNR of 27.57 ± 6.59. BMI was significantly and positively associated with AEC-selected mAs, whereas mAs showed a moderate negative association with liver ROI-based SNR and no significant association with image noise. The negative mAs–SNR association warrants cautious interpretation, because the calculated SNR depends on both liver CT attenuation and image noise. Furthermore, the low coefficient of determination ($R^2 = 0.2189$) indicates that mAs alone is insufficient to explain the variation in quantitative CT image quality under AEC operation. Patient-related characteristics and AEC behavior should therefore be taken into account when CT image quality is evaluated in routine bone scan SPECT/CT examinations.

ACKNOWLEDGEMENT

The authors gratefully acknowledge Dr. M. Djamil Hospital, Padang, for facilitating this research.

AUTHOR CONTRIBUTIONS

Conceptualization, F.R. and A.M.; methodology, F.R. and A.M.; software, F.R., A.M. and Y.D.; validation, F.R. and A.M.; formal analysis, F.R. and A.M.; investigation, F.R. and A.M.; resources, Y.D.; data curation, F.R. and A.M.; writing-original draft preparation, F.R.; writing-review and editing, F.R. and A.M.; visualization, F.R.; supervision, A.M.; project administration, F.R.; funding acquisition, F.R. All authors have read and agreed to the published version of the manuscript.

FUNDING

This research was funded by the Indonesia Endowment Fund for Education (LPDP), Ministry of Finance of the Republic of Indonesia.

DATA AVAILABILITY STATEMENT

The data supporting the findings of this study were obtained from the SPECT/CT computer system at Dr. M. Djamil Hospital, Padang, Indonesia. Due to patient confidentiality and ethical restrictions, the original clinical data are not publicly available. The data supporting the findings of this study are available from the corresponding author upon reasonable request, subject to approval by the relevant institutional authorities and applicable ethical regulations.

CONFLICTS OF INTEREST

The authors declare no conflict of interest.

ARTIFICIAL INTELLIGENCE (AI) USAGE DECLARATION

During the preparation of this work, the author(s) used ChatGPT (OpenAI) for language improvement, translation, and assistance in organizing the manuscript. After using this tool/service, the author(s) reviewed and edited the output as needed and take full responsibility for the content of the publication.

REFERENCES

Alezzi, M., Kotbi, O., Hammid, G., Fouda, A., & Zabarmawi, Y. (2026). Optimization of CT parameters to reduce radiation dose in SPECT/CT bone scans while preserving diagnostic quality. *Applied Radiation and Isotopes*, *231*, 1–7. https://doi.org/10.1016/j.apradiso.2026.112524

Alrehily, F., & Alshamrani, A. F. (2023). Estimation of radiation dose associated with bone SPECT/CT and establishing local diagnostic reference levels using size-specific dose estimate. *Journal of Radiation Research and Applied Sciences*, *16*. https://doi.org/10.1016/j.jrras.2023.100527

Anthon, R., Intifadhah, S. H., & Putri, E. R. (2025). Radiation dose and image quality of bladder cancer patients analysis on abdominal CT-Scan examinations. *Atom Indonesia*, *51*(1), 27–33. https://doi.org/10.55981/aij.2025.1526

Arjah, H., Osman, N. D., Almasri, H., Anam, C., & Aziz, M. E. (2026). Image quality assessment of Hybrid Statistical Iterative Reconstruction (H/SIR) in comparison to Filtered Back Projection (FBP). *Atom Indonesia*, *52*(1), 23–28. https://doi.org/10.55981/aij.2026.1528

Bartel, T. B., Kuruva, M., Gnanasegaran, G., Beheshti, M., Cohen, E. J., Weissman, A. F., & Yarbrough, T. L. (2018). SNMMI procedure standard for bone scintigraphy 4.0. *Journal of Nuclear Medicine Technology*, *46*(4), 398–404.

Ben-Rejeb, N., & Ben-Sellem, D. (2022). Estimation of additional dosimetry from low-dose CT scan to 99mTc-HMDP SPECT/CT. *Journal of Medical Imaging and Radiation Sciences*, *53*(1), 87–92. https://doi.org/10.1016/j.jmir.2021.10.008

Bouchareb, Y., Alsaadi, A., Zabah, J., Jain, A., Al-jabri, A., Phiri, P., Shi, J. Q., Delanerolle, G., & Sirasanagandla, S. R. (2024). Technological advances in SPECT and SPECT/CT imaging. *Diagnostics*, *14*. https://doi.org/10.3390/diagnostics14131431

Dance, D. R., Christofides, S., Mclean, I. D., & Ng, K. H. (2014). *Diagnostic radiology physics: a handbook for teachers and student*. IAEA.

Danielsson, M., Persson, M., & Sjölin, M. (2021). Photon-counting x-ray detectors for CT. *Physics in Medicine & Biology*, *66*, 1–35. https://doi.org/10.1088/1361-6560/abc5a5

Gupta, S. K., Trethewey, S., Brooker, B., Rutherford, N., Diffey, J., & Attia, J. (2017). Radionuclide bone scan SPECT-CT : lowering the dose of CT significantly reduces radiation dose without impacting CT image quality. *American Journal of Nuclear Medicine and Molecular Imaging*, *7*(2), 63–73. PMID: 28533938; PMCID: PMC5435612.

Hoeijmakers, E. J. I., Martens, B., Wildberger, J. E., Flohr, T. G., & Jeukens, C. R. L. P. N. (2025). Objective assessment of diagnostic image quality in CT scans : what radiologists and researchers need to know. *Insights into Imaging*, *16*(154). https://doi.org/10.1186/s13244-025-02037-y

Inoue, Y., Ohkubo, Y., Nagahara, K., Uehara, A., Takano, M., & Dlp, E. D. C. (2022). Conversion from dose length product to effective dose for the CT component of whole - body PET/CT. *Annals of Nuclear Medicine*, *36*(4), 411–419. https://doi.org/10.1007/s12149-022-01720-0

Inoue, Y., Nagahara, K., Kudo, H., & Itoh, H. (2018). Effects of the scan range on radiation dose in the computed tomography component of oncology positron emission tomography/computed tomography. *Radiation Protection Dosimetry*, *185*(1), 1–6. https://doi.org/10.1093/rpd/ncy210

Jaruvongvanich, V., Muangsomboon, K., & Teerasamit, W. (2024). Optimizing computed tomography image reconstruction for focal hepatic lesions : Deep learning image reconstruction vs iterative reconstruction. *Heliyon*, *10*(15), e34847. https://doi.org/10.1016/j.heliyon.2024.e34847

Lee, N., & Joo, M. W. (2025). Current position of nuclear medicine imaging in primary bone tumors. *Diagnostics*, *15*(2786), 1–23. https://doi.org/10.3390/diagnostics15212786

Lin, C., Shen, X., Gu, Y., Qiao, Z., & Peng, W. (2024). A cross-sectional study on the correlation of image quality, effective dose, and body composition with thyroid, chest, and abdominal computed tomography scans. *Quantitative Imaging in Medicine and Surgery*, *14*(6), 4031–4040. https://doi.org/10.21037/qims-23-1731

Martin, C. J., & Sookpeng, S. (2016). Setting up computed tomography automatic tube current modulation systems. *Journal of Radiological Protection*, *36*. https://doi.org/10.1088/0952-4746/36/3/R74

McMillan, K., Bostani, M., Cagnon, C. H., Yu, L., Leng, S., McCollough, C. H., & McNitt-Gray, M. F. (2017). Estimating patient dose from CT exams that use automatic exposure control: Development and validation of methods to accurately estimate tube current values. *Med. Phys*, *44*(8), 4262–4275. https://doi.org/10.1002/mp.12314

Sadia, R. T., Chen, J., & Zhang, J. (2024). CT image denoising methods for image quality improvement and radiation dose reduction. *Journal of Applied Clinical Medical Physics*, *25*, 1–17. https://doi.org/10.1002/acm2.14270

Sookpeng, S., & Butdee, C. (2017). Signal-to-noise ratio and dose to the lens of the eye for computed tomography examination of the brain using an automatic tube current modulation system. *Emerg Radiol*, *24*, 233–239. https://doi.org/10.1007/s10140-016-1470-6

Sookpeng, S., Martin, C. J., Gentle, D. J., & Lopez-Gonzalez, M. R. (2014). Relationships between patient size , dose and image noise under automatic tube current modulation systems. *Journal of Radiological Protection*, *34*, 103–123. https://doi.org/10.1088/0952-4746/34/1/103

Sulayman, M. K., U, F. K., Bashiru, L., Khalis, M., Abdul, K., M, N. A., Kamal, I., C, C. A., R, J. M., & Mazliana, A. K. (2025). Radiation dose of abdominal and lung computed tomography based on body mass index as an indicator. *Malays J Med Sci*, *32*(4), 156–169. https://doi.org/10.21315/mjms-04-2025-280

Tsalafoutas, I. A. (2024). The impact of automatic tube current modulation related settings of a modern GE CT scanner on image quality and patient dose; details do matter. *Journal of Applied Clinical Medical Physical*, *25*, 1–19. https://doi.org/10.1002/acm2.14356

Tulik, M., Tulik, P., & Kowalska, T. (2020). On the optimization of bone SPECT / CT in terms of image quality and radiation dose. *Journal of Applied Clinical Medical Physics*, *21*(11), 237–246. https://doi.org/10.1002/acm2.13069

Vañó, E., Miller, D. L., Martin, C. J., Rehani, M. M., Kang, K., Rosenstein, M., Ortiz-Lopez, P., Mattsson, S., Padovani, R., & Rogers, A. (2017). *Diagnostic Reference Levels in Medical Imaging* (Vol. 46, Issue 1). ICRP Publication 135.

Vaz, S. C., Oliveira, F., & Herrmann, K. (2020). Nuclear medicine and molecular imaging advances in the 21st century. *British Journal of Radiology*, *93*(1110). https://doi.org/10.1259/ bjr. 20200095

Verfaillie, G., Franck, C., De Crop, A., Beels, L., D'Asseler, Y., & Bacher, K. (2023). A systematic review and meta-analysis on the radiation dose of computed tomography in hybrid nuclear medicine imaging. *EJNMMI Physics*, *10*(1). https://doi.org/10.1186/s40658-023-00553-8

Wyngaert, T. Van Den, Strobel, K., Kampen, W. U., & Kuwert, T. (2016). The EANM practice guidelines for bone scintigraphy. *European Journal of Nuclear Medicine and Molecular Imaging*, 1723–1738. https://doi.org/10.1007/s00259-016-3415-4

Yoon, H., Kim, J., Lim, H. J., & Lee, M. J. (2021). Image quality assessment of pediatric chest and abdomen CT by deep learning reconstruction. *BMC Medical Imaging*, *21*(146), 1–11. https://doi.org/10.1186/s12880-021-00677-2

Ziessman, H. A., O'Malley, J. P., & Thrall, J. H. (2014). *The requisites nuclear medicine* (4th ed.). Elsevier.